

# High-Resolution Ultrasound in Research of Mouse Orthotopic Glioma and Ultrasound-Guided Cell Implant

Byung Kook Kwak<sup>1,2</sup>, Jean-Francois H. Geschwind<sup>1,\*</sup>, Pramod P. Rao<sup>1</sup>, Shinichi Ota<sup>1</sup>,  
Romaric Loffroy<sup>1</sup>, MingDe Lin<sup>1</sup>, Shanmugasundaram Ganapathy-Kanniappan<sup>1</sup>,  
Rani Kunjithapatham<sup>1</sup>, Manon Buijs<sup>1</sup>, Labiq H. Syed<sup>1</sup>, Eleni Liapi<sup>1</sup>,  
Vadappuram P. Chacko<sup>1</sup>, Mustafa Vali<sup>1</sup>

<sup>1</sup>Russell H. Morgan Department of Radiology and Radiological Sciences, Johns Hopkins University School of Medicine, North Wolfe Street, Baltimore, USA

<sup>2</sup>Department of Radiology, Chung-Ang University Hospital, Seoul, South Korea

E-mail: [jfg@jhmi.edu](mailto:jfg@jhmi.edu)

Received April 1, 2011; revised April 21, 2011; accepted May 3, 2011

## Abstract

The purpose is to evaluate the feasibility of imaging mouse brain with high resolution ultrasound (HiRes US), and generation of mouse brain tumor (glioma) model under HiRes US guided implantation of glioma cells. Normal mouse brain was imaged with 30 MHz HiRes US in six pups and ten adult nude mice. Glioma model was developed by injecting human glioma cells ( $5 \times 10^5$ ), U-87MG-*luc*, under HiRes US guidance, in three pups and five adult mice. Bioluminescence imaging, magnetic resonance imaging, and HiRes US were used for *in vivo* tumor imaging. In addition, brain imaging *ex vivo* with HiRes US were also performed in three tumor bearing and five normal brains. The brain parenchyma was seen as a homogeneous low echo on HiRes US without locoregional echo differences. An inverted U shaped linear echo structure (fissure) differentiated the telencephalon from the diencephalon. Bilaterally budding structure at the base of the skull represented the trigeminal nerve. The inserted needle, used to implant the glioma cells, was seen as a high linear echogenic reflection. Brain tumor on *ex vivo* HiRes US was well demarcated, homogeneous and hyperechoic compared to the surrounding healthy brain. In conclusion, imaging the brain with HiRes US in small animal model like mouse is possible and convenient. Real-time guiding is possible to perform any intervention from tumor implantation to percutaneous therapeutic procedures. *Ex vivo*, HiRes US is extremely useful to study the detailed anatomical features.

**Keywords:** High-Resolution Ultrasound, Mouse, Brain, Glioblastoma Multiforme, Implant

## 1. Introduction

Ultrasound has not been often used for imaging small animals in research as compared to other *in vivo* molecular imagers such as micro magnetic resonance imaging (microMRI), micro computed tomography (microCT), and optical imagers. Recently, high-resolution ultrasound (HiRes US) machines have been developed, for small animal research [1-4], with fast imaging speed allowing for real-time imaging with a spatial resolution of 15-100  $\mu\text{m}$  and a temporal resolution of XYZ [5-7]. Such HiRes US machine could help researchers acquire not only detailed anatomic images but also be an important tool in precise interventions on small animal organs such as the mouse brain. To the best of our knowledge to date, there

has not been any report on imaging the mouse brain with HiRes US.

Orthotopic implantation of cultured brain tumor cells is highly efficient in generating tumors that are reproducible in terms of growth rate, host time to death, and anatomic location. Stereotactic implantation is considered the gold standard [8,9] with some authors using a special hollow screw for the skull [10]. However, the limited size of the mouse brain and the complex anatomy make location-wise implantation a challenge. Spilling of cells into the cisterns as well as the ventricles cannot be controlled or avoided using current existing techniques, resulting in variable tumor growth rate, host time to death, and anatomic location. Here we demonstrate that under real time HiRes US guidance, U-87MG human



### 2.3. HiRes US Imaging of Normal Brain

Normal brain, of 6 pups (5 to 10 days old) and 10 adult (more than 4 weeks old) mice, was studied by HiRes US (Vevo 2100 system; VisualSonics, Toronto, Canada) equipped with broadband (18 MHz - 38 MHz) mechanical scanning linear array single element transducers (probe MS400; VisualSonics). For this study, the transducers were operated at frequencies of 26 MHz and 30 MHz. A 13 mm in width and 12 mm scanning depth field of view was used. Imaging was done with the animal in the prone position with the transducer in the coronal plane starting at the vortex and moving caudally in a slow, controlled manner. Sagittal imaging was done perpendicular to the coronal imaging starting at the midline and moving laterally on both sides. The machine setting was optimized to obtain a 50  $\mu\text{m}$  resolution with frame rates in 2D up to 628 frames per second (fps) for a  $4 \times 4$  mm field of view, as recommended by the manufacturer (VisualSonics). The images obtained in the coronal plane were then compared and correlated with those of microMRI obtained for the same animal (2 pups and 5 adults) in a similar anatomic plane. The microMRI was used as the reference standard of imaging.

### 2.4. HiRes US-Guided Orthotopic Implantation of Glioma Cells

U-87MG-*luc*, human glioma cells ( $5 \times 10^5$  cells in 5  $\mu\text{l}$  phosphate buffered saline (PBS)/ animal) were injected in to the brains of 3 pups and 5 adult mice, under real time US guidance (Vevo 2100 ultrasound, VisualSonics). In brief, mice were anesthetized with 1.5% - 2% isoflurane mixed with medical air as per the approved animal protocol of Johns Hopkins University Animal Care and Use Committee. The transducer was placed obliquely on the left frontoparietotemporal area with the animal in the prone position. The needle (26 G, 10 mm in length) attached on 50  $\mu\text{l}$  Hamilton syringe (Hamilton, Reno, Nevada) was used for delivering the cells. By free hand ultrasound guidance, the needle was inserted into the brain. The insertion site on the scalp was about 2 mm - 3 mm lateral right to the midline. The syringe was tilted to the right so as to insert the needle at an angle to the transducer in the ipsilateral thalamus under real time visualization of the advancing tip. The prepared cells were injected at a rate of 1  $\mu\text{l}/\text{sec}$ . Burr hole or skin incisions were deemed unnecessary as the needle easily penetrated the skull bone because the bone was very thin. All the procedures were performed under strict aseptic conditions after disinfection of the skin with povidone iodine solution.

### 2.5. Bioluminescence Imaging

For early detection of tumor growth and activity, bioluminescence imaging was used. Bioluminescence was the choice of imaging because of its high sensitivity, easy availability and speed of imaging. A protocol of weekly imaging for four weeks after the date of implant was used. Bioluminescence imaging was performed using a highly sensitive, cooled CCD camera mounted in a light-tight specimen box (Kodak *in-vivo* multispectral imaging system FX; Carestream Health, Rochester, NY), and with Kodak molecular imaging software (Carestream Health). Animals were anesthetized with the induction of 3% isoflurane and the substrate D-luciferin (Gold Bio-Technology) was given by intraperitoneal injection at 150 mg/kg in PBS (Invitrogen, Carlsbad, CA), the mice were then placed in a supine position onto the stage inside the light-tight camera box with continuous exposure to 1.5% - 2% isoflurane. After 5 minutes, bioluminescence acquisition was taken 3 times sequentially for the duration of 5 minutes for each image. Identical illumination settings (f-stop 2.5, field of view 60 mm, binning 8 pixels  $\times$  8 pixels) were used to acquire all images throughout the study. After bioluminescence imaging, white light or x-ray images were taken at the same field of view for image fusion overlay. The displayed bioluminescence intensity scale used was a minimum of 150 units to a maximum of 500 units in all cases.

### 2.6. MicroMRI

MicroMRI of the brain was performed on two normal pup, and three brain tumor bearing and five normal adult mice. For the tumor bearing mice, the microMRI was undertaken within 1 week after tumor detection with bioluminescence imaging. Intracranial tumor was visualized by gadolinium-enhanced microMRI using a 9.4-T, 20 cm horizontal-bore magnet small-animal MRI system (Bruker Biospec, Billerica, MA) equipped with a 40 G/cm gradient coil strength and 35 mm diameter resonator coil. Mice were anesthetized during procedures with 1.5% - 2% isoflurane mixed with medical air. Respiration rate was monitored with an MRI-compatible detection system (SA Instruments, Stony Brook, NY), and kept at 40 - 50 per minute by controlling the isoflurane concentration. High-resolution MR images were acquired with spin echo sequences in the coronal orientation. The parameters for *in vivo* microMRI measurements were as follows: for spin echo images, a fast spin echo sequence with four echoes per excitation for T2 weighted image (WI) and two echoes per excitation for T1WI; matrix,  $256 \times 256$ ; field of view,  $32 \text{ mm} \times 32 \text{ mm}$ ; slice thickness, 0.5 mm; slices, 26 in the coronal plane;

averages, 8 for T1WI, 2 for T2WI; and in-plane resolution, 0.125 mm/pixel; pulse repetition time (TR)/echo time (TE) = 800/8.9 msec for T1 weighted image, 3600/28.7 msec for T2 WI. Contrast enhanced T1WI MRI was taken at the same protocols as non-contrast MRI after injection of 0.2 mmol/kg of MR contrast agent (Magnevist, gadopentetate dimeglumine; Bayer Health-Care, Berlin, Germany) with a 26-gauge needle into the tail vein.

## 2.7. Follow-Up with HiRes US

The mice with tumors confirmed on microMRI as well as bioluminescence were studied using HiRes US with the same imaging parameters described above. The brains of these animals were imaged to evaluate the echo texture, size and site of the tumors. HiRes US imaging was also used to study the secondary effect of the intra-cranial tumors such as hydrocephalus and midline shift if any.

## 2.8. Ex Vivo HiRes US

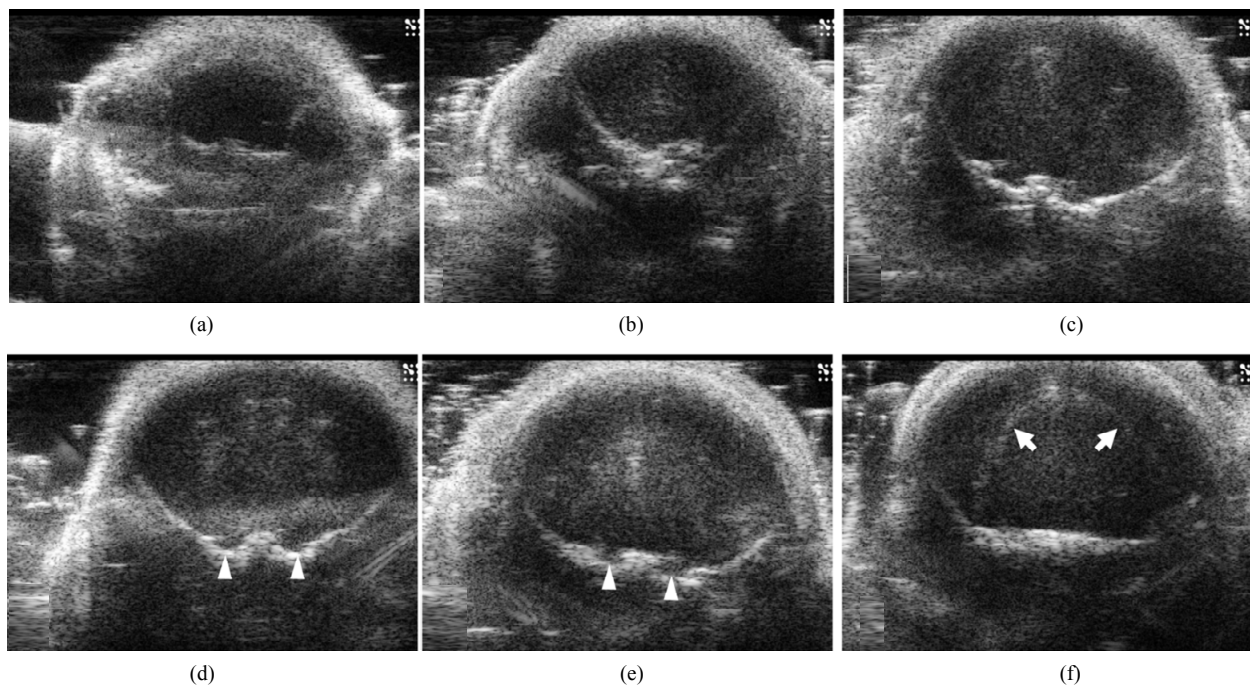
Two normal pups, and three tumor bearing and five normal adult brains were excised and studied with HiRes US. Immediately after sacrifice with CO<sub>2</sub> intoxication, the brains were removed and put on a PBS-containing 10-mm cell culture dish, and images were taken. The HiRes US imaging parameters were maintained as described above. Imaging of the normal and tumor bearing brain *ex vivo* was used to compare them with *in vivo* live images and microMRI images.

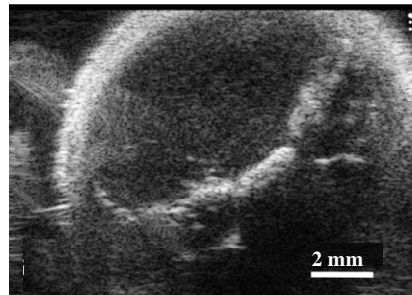
## 2.9. Histopathology

All animals imaged were euthanized by CO<sub>2</sub> intoxication and the brain was carefully dissected out after making an incision on the scalp and separating the skull bones with small forceps. The brain specimen was then cut into 2mm thick slices using a razor blade and a precision brain matrix. These axial slices were then fixed in 10% formalin (Polysciences Co., Warrington, PA), dehydrated by graded ethanol, embedded in Paraplast Plus wax (McCormick Scientific), sectioned at 5 microns, mounted on slides and oven dried and deparaffinized. The tissue sections were subjected to hematoxylin and eosin (H & E) staining. The microscopic images of the tumor and the surrounding normal parenchyma were evaluated and compared with those of microMRI and HiRes US.

## 3. Results

In pups, the brain parenchyma was seen as a homogeneous low echo on HiRes US (**Figure 2**). There were no differences in the echo textures between white and gray matter, cortex and thalami, and fore, mid and hindbrains. The ventricles in these pups were extremely small and collapsed, hence were poorly visualized especially in the background of the low level echoes of the parenchyma. This was comparable with the microMRI images obtained. A well demarcated inverted U shaped linear echo structure differentiated the telencephalon from the diencephalon. That linear echo structure is a fissure formed by the folding telencephalon over diencephalon during





(g)

**Figure 2.** Ultrasound images of coronal scan of 6-day-old mouse brain by 30-MHz high-resolution ultrasound. The brain parenchyma is seen with homogeneous low echo without tissue differentiation (a-g). The ventricles are not visualized. At the base of the brain, pairs of small round echoes (arrow heads) are the trigeminal nerves (d,e). An inverted U shape linear echo (arrows) is well demarcated representing the fissure between telencephalon and diencephalon (f).

embryonic development. Further correlation between microMRI images and the microscopic (H & E) slides revealed the fissure to be an extension of the cerebrospinal fluid (CSF) space (**Figure 2(f)**). Extra axially bilaterally budding structure at the base of the skull adjacent to the pons represented the trigeminal nerve extending in its normal anatomic course (Foramen rotundum and ovale are their exits to extracranial innervation) (**Figures 2(d)**, **(e)**). With the maturation of the skull bones the parenchyma low level echoes seen in pups were further attenuated, however the inverted U shaped linear echo structure was reduced in echo, but still well visualized (**Figure 3**) and the ventricles were not visualized.

The needle was seen as a high linear echogenic reflection in both pups and adult mice (**Figure 4**). The inserted needle tip and shaft could be seen and accurately localized to the site of intended cell implantation. At the beginning of cell injection, any spilled cells with PBS could be monitored in real-time and seen as with higher echo. The inverted U shaped linear echo described earlier can be used as a point of reference for interventions or to localize intra cranial lesions (**Figures 2(f)** and **3**).

Using HiRes US-guided implantation of brain cancer cell lines; orthotopic brain tumors were grown in five mice among eight mice implanted. In five mice, tumor growth was identified after 6-7 weeks from the date of implantation (**Figures 5**, **6**). However, the echo textural differences between the normal brain and tumor on *in vivo* imaging were subtle (**Figure 5(a)**). This can be attributed to the maturation of the skull as described earlier. *Ex vivo* HiRes US revealed excellent differentiation between normal brain parenchyma and the tumor. Brain tumor on *ex vivo* HiRes US was well demarcated, homogeneous and hyper echogenic compared to the surrounding brain. Mass effects like mid-line shifting were seen in one mouse with a big tumor (**Figure 6**) however the dilatation of ventricles was not seen.

Bioluminescence imaging and microMRI both dem-

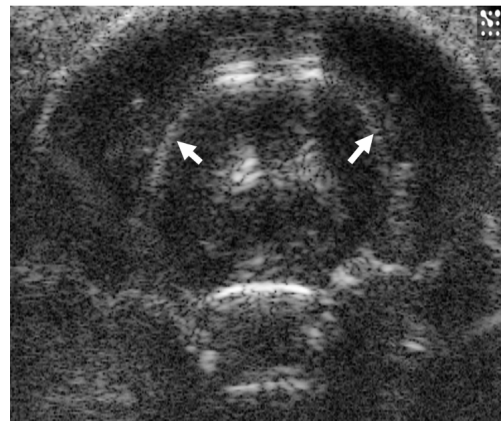


**Figure 3.** Ultrasound image of a fissure between telencephalon and diencephalon by 30-MHz high-resolution ultrasound. In 6-week-old adult mice, parenchymal low echo is much more decreased probably because of the maturation of the skull that attenuated the sound. The inverted U shape linear echo (arrows) between telencephalon and diencephalon is still well demarcated when compared with **Figure 2(f)**.



**Figure 4.** Ultrasound image of needle in brain parenchyma by 30-MHz high-resolution ultrasound. In 6-day-old mouse, 26G needle (arrows) for implant of cancer cells is clearly seen.

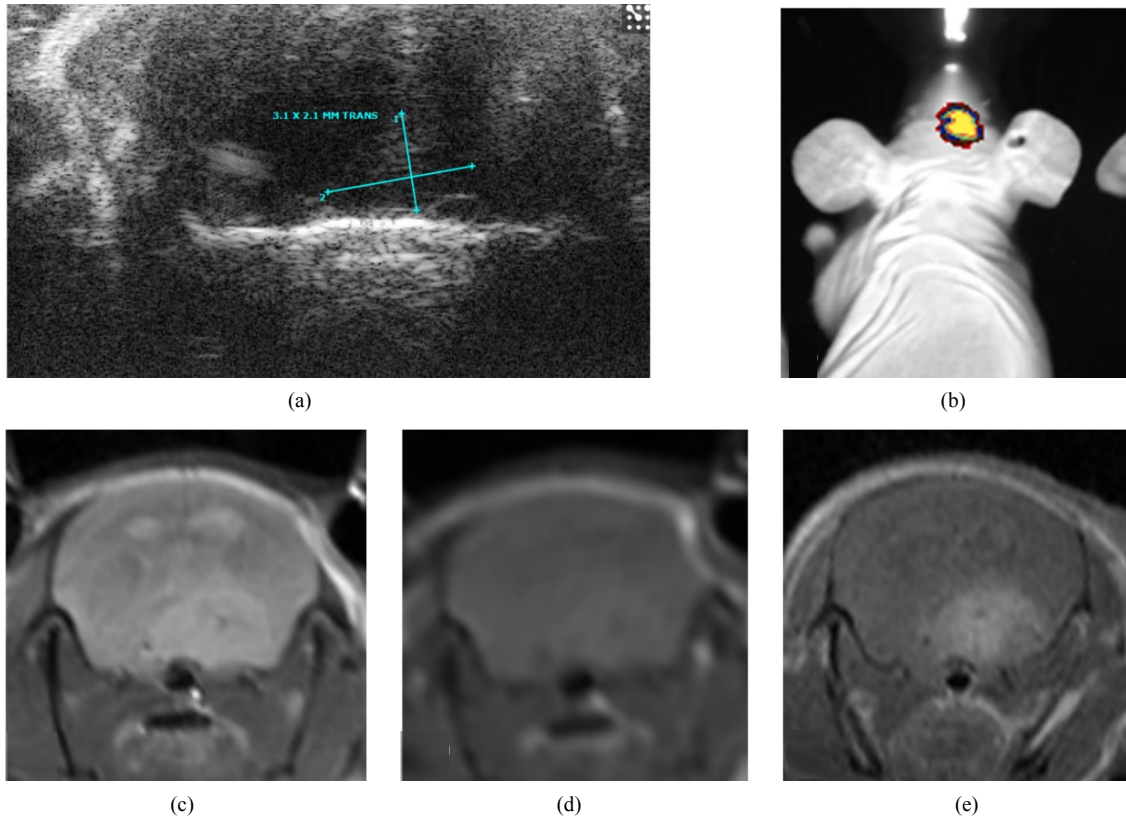


**Figure 5.** Images of orthotopic brain glioblastoma multiforme of mouse. In the 12-week old mouse the brain orthotopic tumor (being measured) is not well visualized on sonographic image by 30-MHz high-resolution ultrasound (a). On optical (b) and MRI (c, d, e) images, the tumor is identified. T2 weighted image (c), non-enhanced T1 weighted image (d) and enhanced T1 weighted image (e).

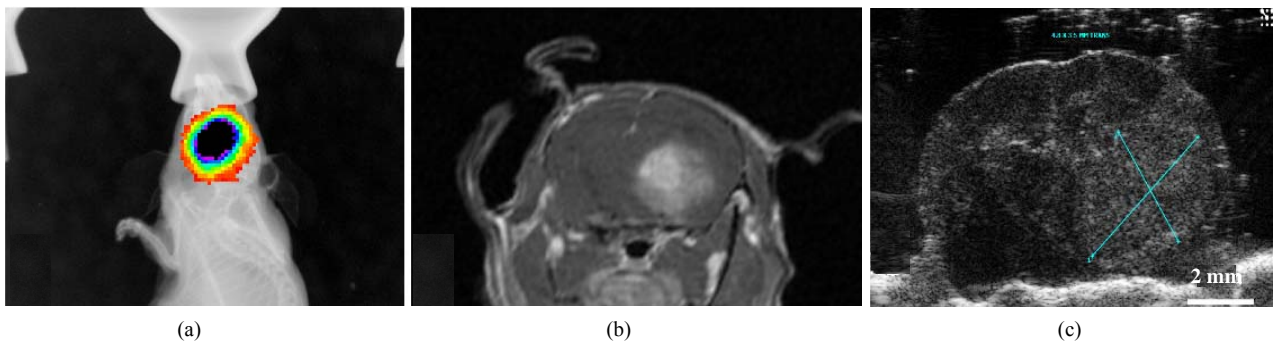


**Figure 6.** Images of orthotopic brain glioblastoma multiforme of 11-week old mouse. On optical (a) and enhanced T1 weighted image (b), the tumor is clear and hyper enhanced in the region of right thalamus. Midline shifting to left by mass is seen. On the ultrasound image (c) of the *ex vivo* brain, increased hyperechoic tumor (being measured) is clearly demarcated with mass effect by 30-MHz high-resolution ultrasound.

onstrated U-87MG growth confirming the feasibility of US-guided orthotopic implantation of glioma cells. Bioluminescence imaging was extremely sensitive for tumor presence and growth detecting tumors as small as 3 mm, however with regards to morphology it could only localize the position with regards to the midline (**Figure 5(a)**). In microMRI, tumor was well demarcated on especially

T2WI and enhanced T1WI sequences. All tumors were highly contrast-enhanced on gadolinium enhanced T1WI (**Figures 5, 6**). Post contrast enhancement on microMRI and photons seen on bioluminescence imaging are highly indicative of disruption of the blood brain barrier in the region of the tumor.

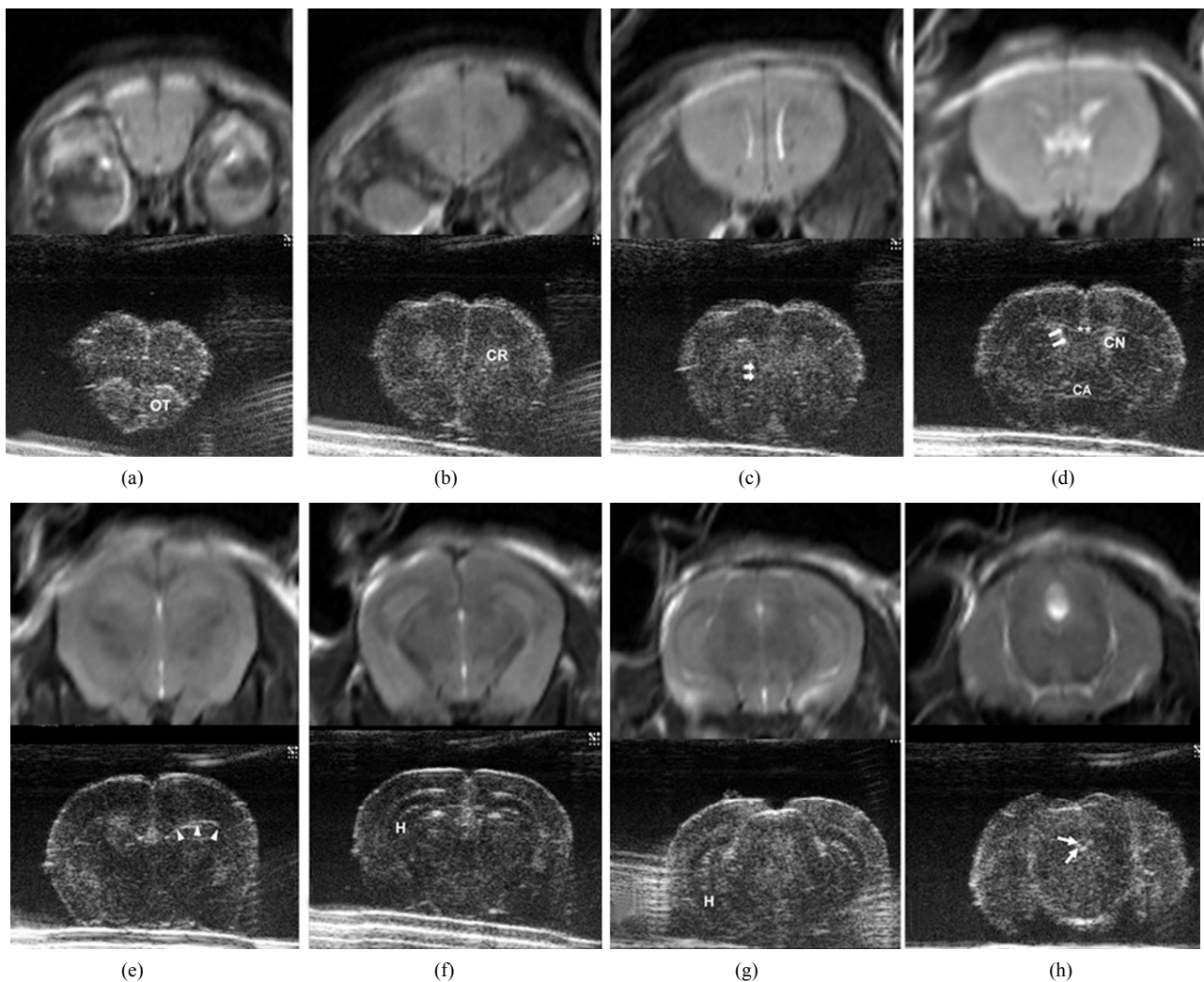
On *ex vivo* HiRes US of normal brain, there was a re-

markable difference noted compared to *in vivo* US imaging, and the structures of the brain very well was demarcated (**Figures 2, 7**). Compared to *in vivo* studies the *ex vivo* HiRes US showed echo textural difference in the different anatomic areas of the brain parenchyma. The interfaces between water and brain parenchyma were relatively thick and hyperechoic on the brain surface and in the ventricles. This thick and hyperechoic outlines might obscure the smaller structures like ventricles. The anterior horns of lateral ventricles (**Figure 7(c)**), aqueduct (**Figure 7(h)**) and 4<sup>th</sup> ventricles (**Figure 7(i)**) were well seen and appeared anechoic. The 3<sup>rd</sup> ventricles and posterior horns of lateral ventricles were not well demarcated. Some structures were extremely well demarcated and delineated. Olfactory track was hyperechoic (**Figure 7(a)**), anterior commissure was linear hypoechoic (**Figure 7(d)**). The fissure between, the cerebral hemispheres (**Figures 7(a)-(f)**), telencephalon and diencephalon (**Figures 7(e), (f)**), and the cerebellometen-

cephalon fissures (**Figure 7(j)**) were prominently hyperechoic. Hippocampus was well delineated appearing hypoechoic (**Figures 7(f), (g)**).

#### 4. Discussions

Ultrasound has many inherent merits like easy accessibility, no radiation hazard, good tissue and water characterization, and real-time observation. Additionally high resolution could be added to these merits. High-frequency ultrasound with more-than-20 MHz transducer is an attractive means of obtaining fine-resolution images of biological tissues for small-animal imaging applications [5-7]. Some studies have demonstrated the unique ability of high-frequency ultrasound systems to image tissues or organs for biomedical applications [1-4]. High-frequency ultrasound penetration depth is reduced because of frequency dependent attenuation. And, most current high-frequency ultrasound images have a small



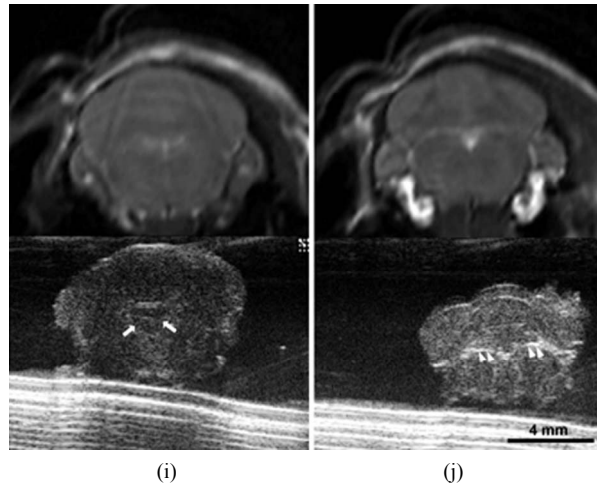


**Figure 7.** Ultrasound images of normal removed brain by 30-MHz high-resolution ultrasound matched with T2 weighted magnetic resonance images. The brain of 12-week-old mouse was removed and put in phosphate buffered saline water dish. From rostral to caudal, anatomical details are clearly seen ((a) - (j)). The interfaces between water and brain parenchyma are hyperechoic on the brain surface and in the ventricles. The ventricles (arrows) are seen well with anechoic in anterior horns of lateral ventricles (c), aqueduct of sylvius (h) and 4<sup>th</sup> ventricle (i). The 3<sup>rd</sup> ventricles and posterior horns of lateral ventricles are not well demarcated. Generally the echoes are similarly hypoechoic in the whole parenchyma. However, there are some echo differences depending on anatomic site in brain parenchyma, which is not as well delineated in the *in vivo* state (Figure 2). Some structures are marked: olfactory tract (OT), corona radiata (CR), double arrows (ventricles), double asterisk (corpus callosum), anterior commissure (CA), caudate nucleus (CN), triple arrow heads (a fissure between telencephalon and diencephalon), hippocampus (H), arrows (a part of ventricles) and double arrow heads (cerebellometencephalon).

depth-of-field. Therefore, typical high-frequency ultrasound images have fine resolution only at shallow depths and over a limited depth-of-field [11,12].

To the best of our knowledge until now there is no report on the imaging of mice brain with such type of ultrasound equipment. The pup's skull is soft enough to study their brain with ultrasound. In adult mice, because of the change in skull density like ossification, the penetration of sound is lesser than in pups, thus the echo information of brain parenchyma is reduced. The mouse brain has homogeneous low echo, so we can know the fact that there is not much difference in tissue density. Internal structure or lobes of brain is not delineated well in the *in vivo* state. Even if there are fluid structures like ventricles, the ventricles are not delineated in the normal brain. That is probably due to these normally being small and collapsed, and the difference in the echo texture between the ventricles and the hypoechoic brain parenchyma is very marginal on *in vivo* imaging. Meanwhile, an extension of CSF space at the fissure between telencephalon and diencephalon was well demarcated as a higher echoic inverted U shaped line (Figures 2(f), 3, 7(e)). For localization of a lesion or intervention, this linear echo a partition line between telencephalon and diencephalon could be used as a landmark. That is, lower (ventral) inner site is the diencephalon, upper (dorsal) outer site is the telencephalon. In adult mouse, brain parenchymal echo is reduced, but the linear echo remains

remarkable (Figure 3).

Real-time observation makes it possible to do a procedure such as inserting a needle, doing a biopsy, implanting cells or infusing a drug at a special functioning site (Figure 4). In a small animal study, doing a procedure for internal tissue or organ is regarded as the unique function of ultrasound when compared with other *in vivo* small animal imagers. Ultrasound is considered the modality of choice for image-guided intervention, which is difficult to be done by any other imaging modalities.

Once implanted tumor cells will develop into tumors, the growth pattern and time will depend on the type of cell line used and the quantity of cells implanted. It takes about 4 - 8 weeks for tumors to develop after the cells have been implanted. Pups implanted with tumor cells grew into adults by the time the tumor grows into a respectable size. In view of the marginal difference between the echoes textures of the tumors and the surrounding brain parenchyma, we recommend another imaging modality like microMRI [13] or optical imaging [14] to be performed along with HiRes US. These additional techniques will help in early detection of tumors and to track changes in the tumors (Figures 5, 6).

In our study, a 26 G needle was inserted into the brain without a burr hole. We found that the needle penetrated the mouse skull without much difficulty. We also observed that there was no difference in the image quality acquired with regards to the anatomic location of imag-

ing (vertex or temporal) of HiRes US. Considering the relatively large size of the transducer compared to the mouse brain, once it was positioned obliquely, one could image a large portion of the mouse brain. This is extremely helpful while doing interventions to use landmarks as well as to monitor the adjacent structure without any loss of image quality or resolution. We did not use a stereotactic system and our procedures were performed by trained radiologists. However, we believe if this system was used along with a stereotactic system or an automatic injector and guiding system sold by some manufacturers it would only enhance the accuracy especially for persons not experienced to the free hand technique.

*Ex vivo* imaging could play an important role especially in studies where percutaneous treatment techniques are used. The *ex vivo* imaging can be used to track the needle tract, to observe post therapy changes in the tumor and adjacent parenchyma and compare it with histopathology. It will also be helpful in marking out the areas for histopathological slides preparation. At the same time one can observe the changes in the brain overall including midline shift, overall we feel this will enhance data collection. If there is a comparison of ultrasound images, *in vivo* and *ex vivo*, with special pathologic staining, each structural echo patterns can be documented.

In conclusion, imaging the brain with HiRes US is possible and convenient in pups, but not much in the adult. Real-time guiding is possible to do any intervention from tumor implantation to percutaneous therapeutic procedures. *Ex vivo* ultrasound is extremely useful to study the detailed anatomy, post procedural change in the tumors as well as the adjacent structures. This we feel will help in accurate specimen sampling as well as increasing the overall data collection quality.

## 5. References

- [1] L. Zhang, X. Xu, C. Hu, *et al.*, "A High-Frequency, High Frame Rate Duplex Ultrasound Linear Array Imaging System for Small Animal Imaging," *IEEE Transactions on Ultrasonics, Ferroelectrics and Frequency Control*, Vol. 57, No. 12, 2010, pp. 1548-1557. [doi:10.1109/TUFFC.2010.1585](https://doi.org/10.1109/TUFFC.2010.1585)
- [2] M. E. Loveless, X. Li, J. Huamani, *et al.*, "A Method for Assessing the Microvasculature in a Murine Tumor Model Using Contrast-Enhanced Ultrasonography," *Journal of Ultrasound in Medicine*, Vol. 27, No. 12, 2008, pp. 1699-1709.
- [3] M. Saar, C. Körbel, V. Jung, *et al.*, "Experimental Orthotopic Prostate Tumor in Nude Mice: Techniques for Local Cell Inoculation and Three-Dimensional Ultrasound Monitoring," *Urologic Oncology*, 2010 (in Print).
- [4] M. W. Laschke, C. Körbel, J. Rudzitis-Auth, *et al.*, "High-Resolution Ultrasound Imaging: A Novel Technique for the Noninvasive *in Vivo* Analysis of Endometriotic Lesion and Cyst Formation in Small Animal Models," *American Journal of Pathology*, Vol. 176, No. 2, 2010, pp. 585-593. [doi:10.2353/ajpath.2010.090617](https://doi.org/10.2353/ajpath.2010.090617)
- [5] N. Hozumi, R. Yamashita, C. K. Lee, *et al.*, "Time-Frequency Analysis for Pulse Driven Ultrasonic Microscopy for Biological Tissue Characterization," *Ultrasonics*, Vol. 42, No. 1-9, 2004, pp. 717-722. [doi:10.1016/j.ultras.2003.11.005](https://doi.org/10.1016/j.ultras.2003.11.005)
- [6] K. Shung, J. Cannata, M. Q. Zhou, *et al.*, "High Frequency Ultrasound: A New Frontier for Ultrasound," *Conference Proceedings—IEEE Engineering in Medicine and Biology Society*, 2009, pp. 1953-1955.
- [7] J. Mamou, O. Aristizábal, R. H. Silverman, *et al.*, "40-MHz Ultrasound Imaging with Chirps and Annular Arrays," *Conference Proceedings—IEEE Engineering in Medicine and Biology Society*, 2008, pp. 2518-2521.
- [8] Q. Xie, R. Thompson, K. Hardy, *et al.*, "A Highly Invasive Human Glioblastoma Pre-Clinical Model for Testing Therapeutics," *Journal of Translational Medicine*, Vol. 6, 2008, pp. 77-90. [doi:10.1186/1479-5876-6-77](https://doi.org/10.1186/1479-5876-6-77)
- [9] Y. K. Hong, D. S. Chung, Y. A. Joe, *et al.*, "Efficient Inhibition of *in Vivo* Human Malignant Glioma Growth and Angiogenesis by Interferon-Beta Treatment at Early Stage of Tumor Development," *Clinical Cancer Research*, Vol. 6, 2000, pp. 3354-3360.
- [10] J. J. Verhoeff, L. J. Stalpers, A. W. Coumou, *et al.*, "Experimental Iodine-125 Seed Irradiation of Intracerebral Brain Tumors in Nude Mice," *Radiation Oncology*, Vol. 2, 2007, pp. 38-45. [doi:10.1186/1748-717X-2-38](https://doi.org/10.1186/1748-717X-2-38)
- [11] S. Sirsi, J. Feshitan, J. Kwan, *et al.*, "Effect of Microbubble Size on Fundamental Mode High Frequency Ultrasound Imaging in Mice," *Ultrasound in Medicine and Biology*, Vol. 36, No. 6, 2010, pp. 935-948. [doi:10.1016/j.ultrasmedbio.2010.03.015](https://doi.org/10.1016/j.ultrasmedbio.2010.03.015)
- [12] A. Stokvis, J. W. Van Neck, C. F. Van Dijke, *et al.*, "High-Resolution Ultrasonography of the Cutaneous Nerve Branches in the Hand and Wrist," *Journal of Hand Surgery (European Volume)*, Vol. 34, No. 6, 2009, pp. 766-771.
- [13] D. Purger, T. McNutt, P. Achanta, *et al.*, "A Histology-Based Atlas of the C57BL/6J Mouse Brain Deformably Registered to *in Vivo* MRI for Localized Radiation And Surgical Targeting," *Physics in Medicine and Biology*, Vol. 54, No. 24, 2009, pp. 7315-7327. [doi:10.1088/0031-9155/54/24/005](https://doi.org/10.1088/0031-9155/54/24/005)
- [14] E. B. Dinca, J. N. Sarkaria, M. A. Schroeder, *et al.*, "Bioluminescence Monitoring of Intracranial Glioblastoma Xenograft: Response to Primary and Salvage Temozolomide Therapy," *Journal of Neurosurgery*, Vol. 107, No. 3, 2007, pp. 610-616. [doi:10.3171/JNS-07/09/0610](https://doi.org/10.3171/JNS-07/09/0610)